WATER EXCHANGE IN PLANT TISSUE STUDIED BY PROTON NMR IN THE PRESENCE OF PARAMAGNETIC CENTERS

GORAN BAČIĆ
*Institute of Physical Chemistry, Faculty of Science, University of Belgrade,
11001 Belgrade, Yugoslavia*

SLOBODAN RATKOVIĆ
*Department of Technology and Chemical Research, Maize Research Institute,
11080 Zemun-Belgrade, Yugoslavia*

ABSTRACT The proton NMR relaxation of water in maize roots in the presence of paramagnetic centers, Mn^{2+}, $Mn\text{-}EDTA^{2-}$, and dextran-magnetite was measured. It was shown that the NMR method of Conlon and Outhred (1972, *Biochem. Biophys. Acta.*, 288:354–361) can be applied to a heterogenous multicellular system, and the water exchange time between cortical cells and the extracellular space can be calculated. The water exchange is presumably controlled by the intracellular unstirred layers. The $Mn\text{-}EDTA^{2-}$ complex is a suitable paramagnetic compound for complex tissue, while the application of dextran-magnetite is probably restricted to studies of water exchange in cell suspensions. The water free space of the root and viscosity of the cells cytoplasm was estimated with the use of $Mn\text{-}EDTA^{2-}$. The convenience of proton NMR for studying the multiphase uptake of paramagnetic ions by plant root as well as their transport to leaves is demonstrated. A simple and rapid NMR technique (spin-echo recovery) for continuous measurement of the uptake process is presented.

INTRODUCTION

When measuring the labeled water exchange across biological membranes, one is always faced with the problem of unstirred layers on both sides of the cell membrane (1). An NMR method, free from the problem of external unstirred layers, was introduced by Conlon and Outhred (2) to measure the water exchange time (τ_a) between erythrocytes and blood plasma. The cells were put into a solution of paramagnetic ions, and the enhancement of the relaxation rate of intracellular water was dependent on the water exchange rate across the cell membrane. Recently, different NMR methods were shown for the evaluation of the τ_a in several cellular systems (3). Most NMR studies on water exchange have been done on erythrocytes (4) or on single-celled algae (5, 6). The vacuolated plant cells with cell walls appear to be more complicated experimental subjects for such studies than animal cells, and the problem of external unstirred layers is especially serious in multicellular plant tissue (7). We report here a detailed study of water relations within a complex plant tissue (maize root) using the technique of Conlon and Outhred (2).

Manganese ions (Mn^{2+}) have been used as the paramagnetic relaxation centers in all previous NMR studies of water exchange. It was shown (4) that high manganese concentration can inhibit the water exchange across erythrocyte membranes. We introduce here new relaxation reagents: a manganese complex with ethylene diamino tetra-acetate (Mn-EDTA) and dextran-magnetite (8) as a possible improvement of the method. It was found (9, 10) that metal-EDTA^{2-} complexes could serve as extracellular markers due to their relatively large molecular size and negative charge. Unlike metal ions alone, EDTA complexes are not toxic to plants.

The mechanism of absorption and transport of ions by plants was usually studied employing radioisotopes (11, 12) or atomic absorption spectrophotometry (13, 14). Most of the plant micronutrients (e.g., Mn, Fe, Co) are paramagnetic, which suggests the possibility of introducing NMR or EPR techniques into investigations of micronutrient transport in plants. Proton NMR monitors the translocation of paramagnetic ions indirectly, since we measured the relaxation properties of tissue water affected by the presence of paramagnetic ions, assuming that the enhancement of water relaxation rates is proportional to the intracellular ion concentration.

MATERIALS AND METHODS

Plant Material

Maize seedlings (*Zea mays* L., hybrid ZP SC 46A) were cultured in distilled water according to the procedure previously described (15). 3–4-d old seedlings were used in all experiments.

Preparation of Solutions

A concentrated solution of the Mn-EDTA complex was made as follows. MnCl$_2$ was added to a 0.15 mM Na$_2$H$_2$EDTA to yield the solution with a ligand to metal-ion mole ratio of 1.03:1. The solution was adjusted to the optimum pH equaling 7.5 for the complete formation of a single complex, i.e., Mn-EDTA^{2-}, using a dilute NaOH solution. The final volume was adjusted to yield a 0.1 mM Mn-EDTA solution. Dextran-magnetite (Meito-Sangyo Co., Inc., Tokyo, Japan) was dissolved in a known volume of deionized water to yield ~1.5 × 10^{-6} mM solution (1 mg dextran-magnetite per 1 g of water), i.e., to give a proton spin-lattice relaxation time $T_1 \simeq 8$ ms.

Sample Preparation

A schematic cross-sectional view of a typical root structure is shown in Fig. 1. Experiments of the following type were performed. (a) The roots of intact maize seedlings were soaked in experimental solutions for various times (from a few minutes to 24 h). After soaking, the roots were blotted with paper to remove excess liquid, cut into 1-cm long segments, and T_1, water, and manganese contents determined. In some of the experiments these roots were separated into steles and cortexes and the same parameters for both root parts determined. Steles were separated from primary roots by bending the root at right angles between 4–5 cm from the tip so that the cortex cracked transversely; the steles were then pulled from the cortex.

We attempted to estimate the water-free space (WFS) of the root using Mn-EDTA^{2-}. The WFS is commonly defined as the volume that would be occupied by the substance at the same concentration as in the bathing medium expressed as a percentage of wet weight of the tissue assuming a density of 1 (10). To do that it was necessary to find the volume of the surface film of the solute. Therefore, the roots were immersed in solutions of Mn-EDTA complex (10–50 mM) for 15 s, blotted, and the manganese content of the surface film of the roots determined. It was found (9) that metal chelates do not penetrate the walls of cortical cells to any visible extent during this brief immersion.

(b) The intact seedling was transferred to an NMR tube and a large volume (at least 10 times larger than sample volume) of experimental solutions (MnCl$_2$, 1–50 mM; Mn-EDTA, 10–100 mM; dextran-magnetite 0.0015 mM) was poured over the root. The influx of paramagnetics was followed by changes in relaxation properties (T_1, recovery of spin-echo intensity, and free induction decay (FID) at fixed delay) of the root water.

(c) The root of an intact seedling was exposed to a 50 mM MnCl$_2$ solution and its leaf positioned between the poles of the electromagnet
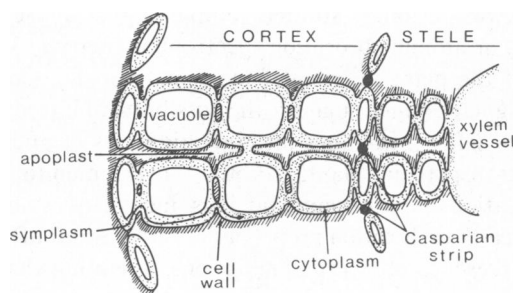

FIGURE 1 Diagrammatic sketch of the root cross section showing linear aggregation of root cells. The root structure can be divided into two well-separated parts: a big cortex section and a smaller inner part called the stele. The number of cells along the root radius is much larger than that shown in this simplified picture. Typical cortical cell radius is ~20 μm (20). A large central vacuole is surrounded by a tonoplast membrane. The outer membrane that bounds the cytoplasm is termed plasmalemma. The terms apoplast and symplasm refer to the cell walls and cytoplasmic continuums, respectively, as possible transport pathways for water and ions.

(16). The manganese translocation to the shoot from the root was followed by measuring the proton T_1 of water in a leaf.

NMR Measurements

A pulsed coherent NMR spectrometer, model IJS-2-71, operating at 32 MHz was used in all NMR experiments. The proton spin-lattice relaxation time of root samples and external solutions (T_{1e}) was measured using standard 180°—τ—90° pulse sequence. A single exponential decay of magnetization was found for roots in the absence of paramagnetic centers or for solutions of paramagnetic ions. When roots come into contact with solutions of paramagnetic ions (Mn^{2+} or Mn-EDTA^{2-}), we observed a single proton signal from the tissue (T_1') at the beginning of uptake (Fig. 2 A). The fast decaying T_{1e} component can be easily resolved from the tissue proton signal. As the uptake of ions proceeds, the signal from the root becomes nonexponential; a good fit to the data is obtained with two exponentially decaying components T_{1a}' and T_{1b}' (Fig. 2 B).

The value of the fast relaxing component (T_{1a}') was determined by subtracting the slow relaxation component (T_{1b}') from the experimental curve (solid line). When the roots in region B are removed from the external solution, two T_1 components are still present and have nearly the same relaxation times as those in the presence of the solution. Even in region A, the roots themselves display two components. The faster component comes presumably from the water in the extracellular space of the root where the paramagnetic centers are already present. In the presence of the external solution this fast component in region A is not seen presumably because it is overwhelmed by the large T_{1e} signal.

While measurements of T_1 were made throughout the uptake experiments, the other two techniques were used for continuous monitoring of the first phase of uptake. (a) When (90° − τ − 180° − $T)_n$ pulse sequence is applied to a root sample without paramagnetic ions and under condition $T \gg 5T_1$ (T, waiting time; T_1, spin-lattice relaxation time of root water), a normal spin-echo signal is obtained (Fig. 3 A). At a fast repetition rate, i.e., $T = 200$ ms $\ll T_1$, the spin-echo intensity was dynamically suppressed (Fig. 3 B). The pulse spacing, $\tau \geq 20$ ms, was adjusted to be much longer than the ^{1}H spin-spin relaxation time of the external Mn-EDTA solution. Such a choice of parameters, τ and T, enabled complete nulling of the proton spin-echo magnetization at the onset of the experiment. After addition of the Mn-EDTA solution, the Mn-EDTA^{2-} ions started to enter the root and an echo signal appeared due to the shortening of the average T_1 of the root water (Fig. 3 C, D), which was continuously recorded using a signal averager. In fact, immediately after the contact of the root surface with the solution, there was an initial jump of the signal (15–20 s) followed by a much slower process of recovery of the spin-echo intensity. The spin-spin relaxation time of the root water was also affected by the presence of paramagnetic centers, but it seemed that the shortening of the T_1 was more dominant (changes of T_1 and spin-echo intensity within the influx times were identical, Figs. 8 and 9).

(b) The usual 180°-τ-90° pulse sequence for T_1 measurement was applied, and τ adjusted to give the zero amplitude of the FID signal of the tissue water. After addition of the paramagnetic ions, the FID at unchanged τ started to appear due to the shortening of T_1 inside the root. The FID amplitude was recorded every 10 s and the influx curve similar to spin-echo recovery was obtained.

Water Content

The water content was determined by weighing freshly excised samples, drying to constant weight in an oven at 378°K, followed by reweighing.

Manganese Content

The total manganese content of the root segments was determined by atomic absorption spectroscopy with a PYE UNICAM SP-192 atomic absorption spectrophotometer. ~10 mg of dry tissue, pretreated with MnCl$_2$ and Mn-EDTA solutions, were digested in a mixture of mineral
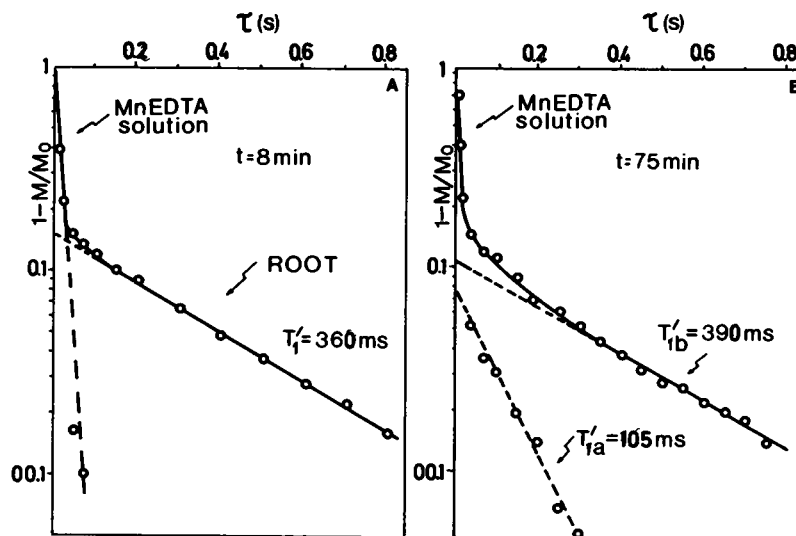
FIGURE 2   Decay of the proton NMR signal $(1 - M/M_o)$ vs. delay time (τ) between pulses for the maize roots measured together with 50 mM Mn-EDTA solution. (A) soaking time, t = 8 min (region A in Fig. 5); (B) soaking time, t = 75 min (region B in Fig. 5). A fast decaying proton signal from external solution (T_{1e} = 7.2 ms) is shown in A. The total magnetization in region B (Fig. 5) is a sum of three components: $M = M_{oe}[1 - 2\exp(-\tau/T_{1e})] + M_{oa}[1 - 2\exp(-\tau/T'_{1a})] + M_{ob}[1 - 2\exp(-\tau/T'_{1b})]$, where M_{oe} and $M_{oa,b}$ are equilibrium magnetizations for water protons in external solution and inside the root, respectively, while T_{1e} and $T'_{1a,b}$ are corresponding relaxation times. The amplitudes P'_a and P'_b are calculated using $P'_a = M_{oa}/M_{oa} + M_{ob}$ and $P'_b = 1 - P'_a$.

acids, dissolved in dilute HCl, and the manganese content was estimated in an acetylene-air flame at wavelength of 279.5 nm. Each sample was a pool of 3–6 roots and analyses were done in triplicate. The manganese content is expressed as micromoles per liter of manganese per gram of tissue fresh weight.
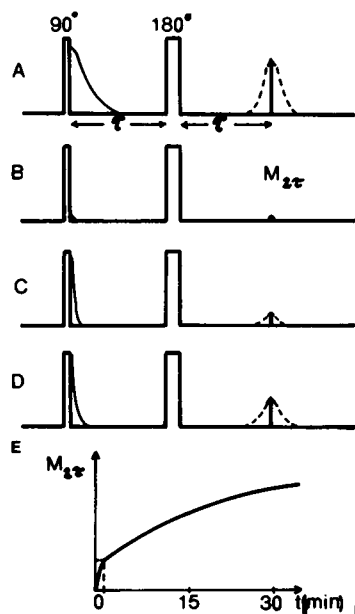

FIGURE 3   Spin-echo recovery technique applied to study influx kinetics of paramagnetic ions to the root. (A) Standard spin-echo sequence used to obtain the proton echo from a root. $T > 5T_1$ and $\tau \geq 20$ ms. (B) Suppression of the proton echo signal from the same sample under condition $T \ll T_1$. (C, D) After addition of the Mn-EDTA solution the echo appears again and its intensity, $M_{2\tau}$, increases with time t (E). The strong FID signals at C and D are from solvent protons that give no echo at $\tau \geq 20$ ms.

RESULTS

The NMR signal of the water protons in the cortex and the stele decayed exponentially (Table I) although there are several compartments of water in both parts of the root (vacuolar, cytoplasmic, and extracellular water). The signal from the non-water protons can be neglected since water represents some 93% of the root fresh weight. Relaxation times of water in the stele and the cortex are directly proportional to the water content of these parts of the root (Table I). However, the proton magnetization induced in the control (in the absence of paramagnetic ions) roots relaxed as a single exponential, indicating a fast exchange (faster than 0.86 s) of water between the different parts of the root.

The two T_1 components of root treated with a solution of paramagnetic ions and measured after removal from the solution, depend identically on the soaking time; only the slow-relaxing one is shown in Fig. 4, b. The manganese contents of the roots and $1/T'_{1b}$ were plotted vs. the square root of time because this enables a contraction of the long

TABLE 1
PROTON SPIN-LATTICE RELAXATION TIME, T_1, OF WATER IN UNTREATED ROOTS OF MAIZE AND CORRESPONDING WATER CONTENT*

	Root	Cortex	Stele‡
Water content	13.4 ± 1.3	14.2 ± 1.4	8.8 ± 0.9
T_1 (s)	1.17 ± 0.05	1.19 ± 0.02	0.86 ± 0.11

Values are mean ± SE (n = 25).
*g H_2O per g dry tissue weight.
‡Stele represents (13 ± 1.5)% of root fresh weight.
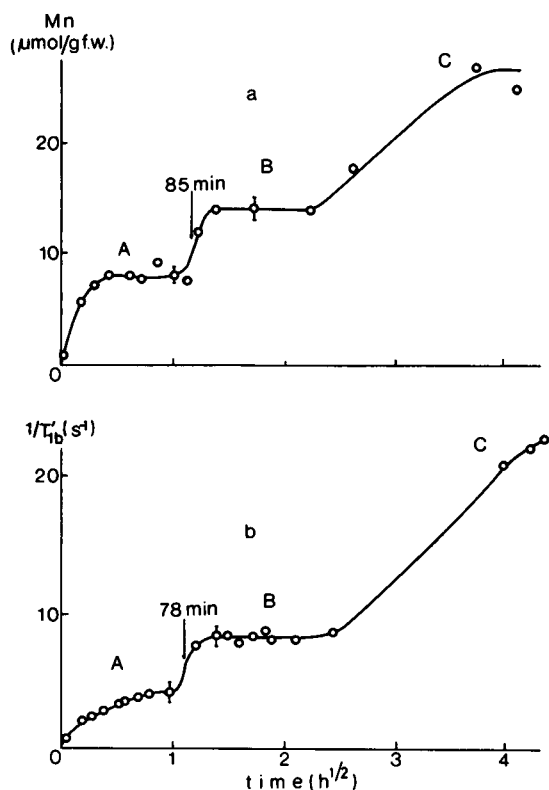
FIGURE 4 (a) Manganese content of the roots treated with 50 mM MnCl$_2$ solution vs. soaking time $t^{1/2}$. (b) Proton relaxation rate, $1/T'_{1b}$, (longer T_1 component) vs. soaking time $t^{1/2}$. The NMR measurements were done after the roots were removed from the solution. Standard error of the mean ($n = 3$–4) is shown for one point in region A and B. The arrows indicate the transition points.

time scale. The complex curves in Fig. 4 can be divided into three well-distinguished regions: A, B, and C. Our experiments show that such a multiphase pattern is a general feature of the absorption process, independent of the nature of the absorption solution (MnCl$_2$ and Mn-EDTA) and of the concentration of solution (1–100 mM).

Changes of T_1 of intracellular water protons of maize roots, in the presence of 50 mM Mn-EDTA and MnCl$_2$ solutions, as a function of time are shown in Figs. 5 and 6, respectively. The two components in region B were observed for external concentrations of Mn-EDTA and MnCl$_2$ higher than 25 and 5 mM, respectively. Single T_1 was observed for lower concentrations, changing with soaking time in the same manner as shown in Fig. 4. In region A the relaxation rate of water in stelar tissue of treated roots has the same value as in the steles of control roots, but T_1 again splits into two components in region B (Fig. 5). Upper curves in Figs. 5 and 6 show that the moment of T_1 splitting corresponds to the appearance of manganese in the stele as well as to the increase in the manganese content of the cortex. The T_1 of water in roots treated with 1.5 × 10^{-6} mM dextran-magnetite solution was not changed compared with the control roots, even for 20 h of treatment.

Changes in R_1 of water in the maize seedling's leaves soaked in MnCl$_2$ solution are shown in Fig. 7. The value of R_1 is the same as in the leaves of untreated plants ($R_1/R_1^0 = 1$) up to 78 min. The abrupt change in R_1 after this time is obviously a consequence of the manganese influx to the leaf. Note that the appearance of the manganese in leaves coincides with the transition points in Figs. 4 and 6. Fig. 7 also shows that once in the stele, manganese is rapidly translocated to the shoot. Transition points for the other concentrations are given in Table II.

Fig. 8 shows the first stage of Mn-EDTA^{2-} uptake (region A) by roots followed by different techniques. The spin-echo recovery technique appears to be very convenient for following the kinetics of the uptake process. The advantages of this technique over T_1 measurements are the following (a) The echo amplitude can be monitored almost continuously (every 200 ms), while for T_1 determination one needs at least 1 min, and (b) this method is free from the problems arising in the curve peeling method in a semi-logarithmic plot.

Analysis of the results obtained with the spin-echo recovery technique revealed the existence of one very fast process that is completed within 15–20 s (not shown in Fig.
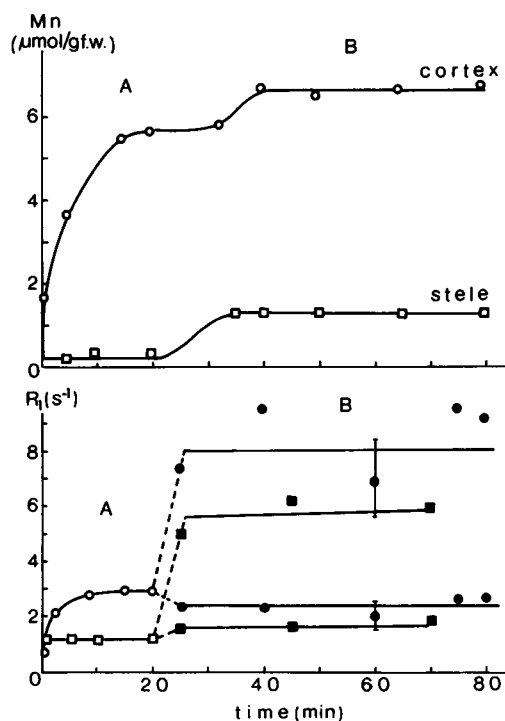

FIGURE 5 Comparison of the manganese content of the root and relaxation rate of tissue water protons for roots treated with 50 mM Mn-EDTA for different times. Upper curves: manganese content of cortex (o) and stele (□). Lower curves: spin-lattice relaxation rate, R_1, of intact root (o) ans stele (□). Region A, single exponential T_1 decay (o, □); region B, biexponential T_1 decay (●, ■). The relaxation from the root was measured in the presence of the external solution. The measured amplitudes of fast and slow relaxing component are $P'_a = 0.32 \pm 0.05$ and $P'_b = 0.618 \pm 0.05$, respectively.
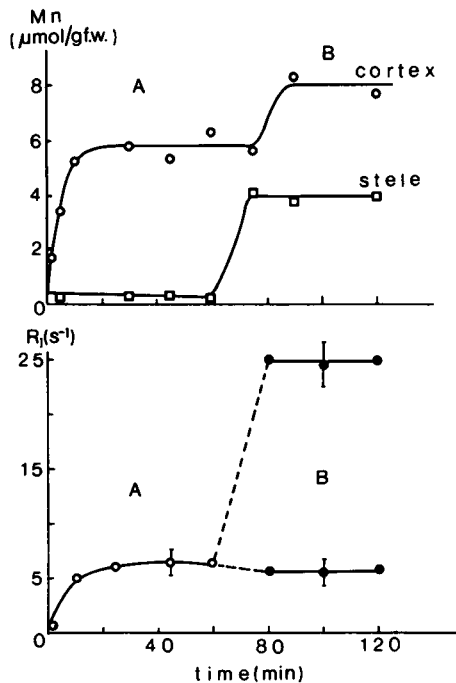
FIGURE 6 Comparison of the manganese content of the roots and relaxation rate of tissue water protons for roots treated with 50 mM MnCl₂ for different times. *Upper* curves: manganese content of cortex (o) and stele (□). *Lower* curves: spin-lattice relaxation rate R_1 of intact root measured together with MnCl₂ solution. Region A, single exponential T_1 decay (o); region B, biexponential T_1 decay (●). The measured amplitudes of the fast and slow relaxing components are 0.35 and 0.65, respectively.

8). The 15–20 s time lag is necessary for the saturation of the surface film of the root with paramagnetic ions, and this initial jump of the echo amplitude is a result of the contact between the root surface cells and paramagnetic ions. The rest of the influx process can be fitted to a single
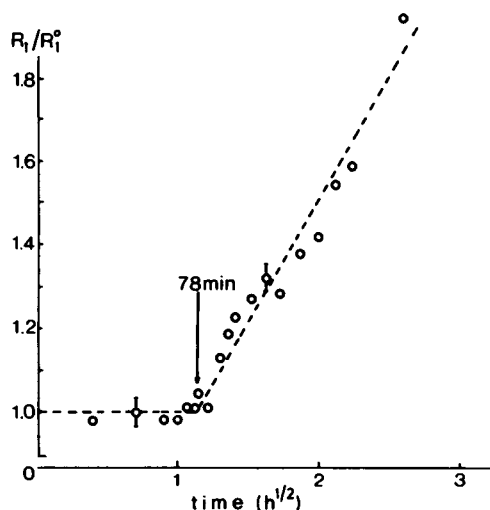

FIGURE 7 Normalized value R_1/R_1^0 of the relaxation rate of water in leaves ($n = 3$) of maize seedlings exposed to 50 mM MnCl₂ vs. square root of soaking time. R_1-treated, R_1^0-control. The arrow indicates the transition point.

TABLE II
MANGANESE UPTAKE INTO MAIZE ROOTS AS A FUNCTION OF CONCENTRATION OF ABSORPTION SOLUTION

Solution	Concentration	Manganese content* μmol/g F.W.		Transition point
		A	B	
	mM			*min*
MnCl₂	10	2.5 ± 0.3	3.7 ± 0.2	85 ± 10
	25	3.8 ± 0.3	5.8 ± 0.3	80 ± 10
	50	6.9 ± 1.1	11.0 ± 3.0	85 ± 10
Mn-EDTA	10	0.7 ± 0.1 (0.5 ± 0.1)	1.0 ± 0.2	160 ± 15
	25	2.3 ± 0.6 ‡ (1.5 ± 0.6)‡	3.3 ± 0.3	120 ± 10
	40	3.8 ± 0.3 (3.0 ± 0.4)‡	4.5 ± 0.4	70 ± 10
	50	5.2 ± 0.3 (3.5 ± 0.4)‡	5.6 ± 0.3	35 ± 5
	75	15.0 ± 1.0	21.0 ± 2.0	25 ± 5

*Saturation values in region A and region B, respectively (see Fig. 4).
‡Corrected for the amount of manganese in surface film of the root.

exponential function: $C_t = C_\infty(1 - \exp[-kt])$, where C_t is the concentration of manganese in the root at any time, t, C_∞ is the saturation value on the plateau, and k is rate parameter. Halftimes, $t_{1/2}$, for this process were calculated from the slope $\ln(1 - C_t/C_\infty)$ vs. t for different concentra-
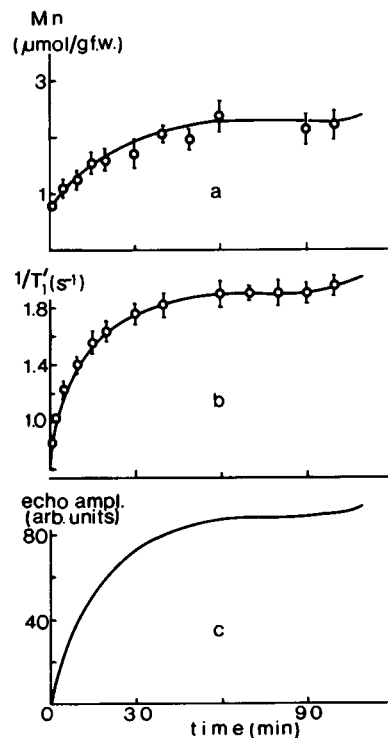

FIGURE 8 Initial uptake of manganese by maize roots from 25 mM solution of Mn-EDTA followed by (*a*) atomic absorption spectroscopy, (*b*) proton relaxation rate of tissue water (exponential T_1 decay) and (*c*) recovery of the spin-echo amplitude.

tions of the external Mn-EDTA solutions. Fig. 9 shows that values of $t_{1/2}$ calculated from spin-echo recovery experiments agree well with the values estimated from other experiments, and that $t_{1/2}$ is an exponential function of the concentration of Mn-EDTA.

It is generally accepted (9, 18) that the initial stage of entry is the free diffusion of solute from the surroundings of the plant root into the free space, and it seems (see Discussion) that region A corresponds to the influx of Mn-EDTA^{2-} into the root apoplast. Negative charge of the complex prevents binding to fixed negative charges in the cell walls, and the binding constant of EDTA is several orders of magnitude greater for Mn than for Ca or Mg (17). Therefore, the apparent water-free space of the root can be calculated from the saturation values of the manganese content. Using the manganese content corrected for the amount of manganese in the surface film (values in parentheses in Table II), we estimate the WFS to be 7.0 ± 1.0% of wet tissue weight as an average for all concentrations of Mn-EDTA solutions used. Some absorption of Mn-EDTA^{2-} within the extracellular space may take place, but its contribution to the estimation of WFS is most probably reduced due to the relatively high concentrations of the marker. The stele, into which Mn-EDTA^{2-} did not readily diffuse, occupies 13% of the root tissue (Table I). The free space of the cortex, therefore, occupies 8.0% of the tissue. This value is comparable with the 5.4% calculated for wheat root (9), using the electron microscope with Pb-EDTA as an extracellular marker.

DISCUSSION

NMR measurements of water exchange across biological membranes that use paramagnetic ions are based on an assumption that these ions do not significantly enter the cells within the time scale of the measurements. If this
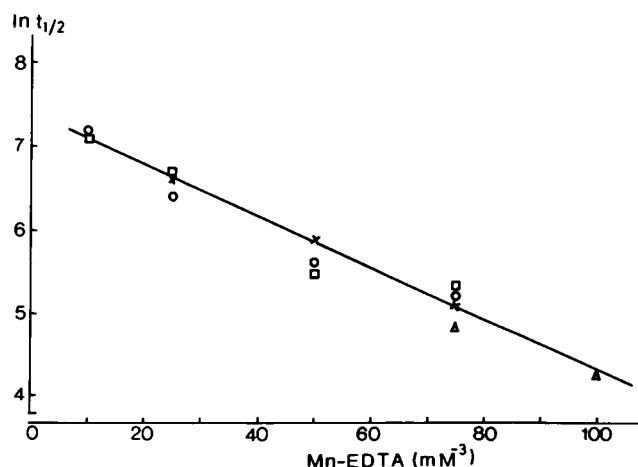

FIGURE 9 Natural logarithm of half-times $t_{1/2}$ for saturation of extracellular space of the maize root with Mn-EDTA^{2-} complex as a function of concentration of the external Mn-EDTA solution. Uptake of Mn-EDTA^{2-} was followed by: T_1' (o), spin-echo recovery (X), FID at fixed delay (△), atomic absorption spectroscopy (□).

NMR method is applied to multicellular systems such as plant root, it is advantageous to saturate the extracellular space of the tissue with paramagnetic ions. Our experiments on manganese uptake revealed a multiphase absorption curve with well-defined plateaus (Figs. 4, 5, and 6). The first phase of uptake that we attribute to the diffusion of ions (Mn^{2+}, Mn-EDTA^{2-}) into the root apoplast (Fig. 1) is considered to be in free diffusional continuity with the external solution (18). The assumption that significant amounts of manganese ions were not entering the cells during that period was supported by the following facts. (a) The manganese ions were not entering the stele in region A (Figs. 5 and 6), and (b) kinetic analysis of the uptake in region A showed that the influx curve, except for the first 15–20 s, could be fitted with a single exponential curve. Similar results were obtained (10) for distribution of ^{60}Co-EDTA^{2-} in the guinea-pig muscles, where 95% of initially accumulated marker followed the bulk diffusion kinetics. However, this is not a simple diffusion since $t_{1/2}$ depends on concentration (Fig. 9). Concentration-dependent diffusion coefficients are often found in heterogeneous systems (19). Some additional experiments on isotopic exchange of Mn-EDTA^{2-} should make this point more clear (manuscript in preparation). (c) In wheat roots treated with Pb-EDTA, the complex was found only in the free space in the initial phase of uptake (9).

If the above assumption is valid, the water exchange time, τ_a, between the cells and the extracellular space can be calculated from the observed spin-lattice relaxation time, T_1 (saturation values in region A) of intracellular water in the presence of paramagnetic ions outside the cells. A complete description of the theory is given by Pirkle et al. (4) or Stout et al. (6), and τ_a can, therefore, be calculated from equation

$$1/T_1' = 1/T_1 + 1/\tau_a,\qquad(1)$$

where T_1 is the relaxation time of control roots. Eq. 1 is correct only if the relaxation time of extracellular water is short compared with the T_1 and the τ_a, i.e., if a sufficient amount of paramagnetic ions are present in the extracellular space to make the backflux term negligible. Under this condition, T_1' should be independent of the manganese concentration outside the cells. Fig. 10 shows that T_1' depends on the concentration of the external Mn-EDTA solution up to 75 mM, while it is nearly independent of the concentration of MnCl$_2$ solutions. Plotting the proton relaxation rate $(1/T_{1c})$ of external solution instead of the concentration on the abscissa in Fig. 10 enables a better comparison of the relaxation reagents. The observed difference in T_1' between the roots loaded with MnCl$_2$ and Mn-EDTA can be correlated to the manganese concentrations within the extracellular space for both compounds. Table II shows (column A) that at the same external concentrations of paramagnetics, the root will absorb more manganese from MnCl$_2$ than from Mn-EDTA solution, presumably because Mn-EDTA^{2-} is distributed only in
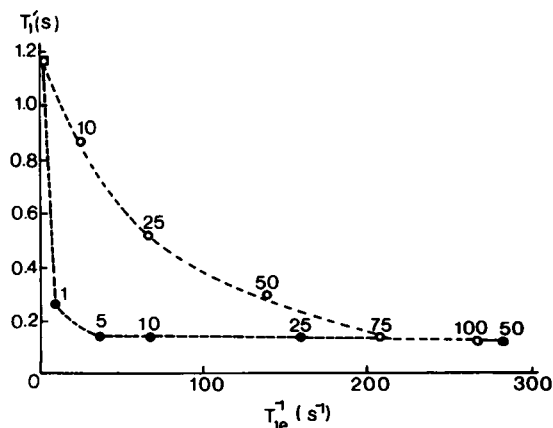
FIGURE 10 The relaxation time of root water T_1' (saturation values in region A in Figs. 5 and 6) vs. relaxation rate of external solution $1/T_{1e}$. Numbers on curves are concentrations of external $MnCl_2$ (●) and Mn-EDTA (○) solutions in mM^{-3}. □, T_1 of control root.

WFS, while Mn^{2+} also binds to cationic exchange sites in the cell walls. We have also calculated the molar longitudinal relaxation enhancement for these solutions and found a 2.5 times higher value for Mn^{2+} than for $Mn-EDTA^{2-}$. The dependence of T_1 on the external concentration of Mn-EDTA at low concentrations, therefore, means that under this condition the water backflux cannot be neglected.

It seems that large molecules of dextran-magnetite did not diffuse to regions of the extracellular space inside the root surface. Therefore, a small fraction of cells was in contact with dextran-magnetite, and the average T_1' did not differ significantly from T_1 of control roots.

At high external Mn-EDTA concentrations, T_1' becomes equal to the value obtained using $MnCl_2$ (Fig. 10). This value, $T_1' = 140 \pm 10$ ms, was used to calculate the water exchange time (Eq. 1) and $\tau_a = 155 \pm 10$ ms was obtained. This is a very high value compared with τ_a obtained for other cells by NMR methods (3). The diffusional water permeability of cell membrane (P_d) can be found if the cell area (A) and the volume (V) are known, and if for cylindrical cells

$$P_d = V/(A\tau_a) = r/(2\tau_a).\qquad(2)$$

Assuming that the radius r of the average cortical cell is 20 μm (20), the typical membrane permeability of these cells to water, $P_d = (6.5 \pm 0.9) \times 10^{-3} \, cm \, s^{-1}$, was found. This is three orders of magnitude higher than calculated for the same system using isotopic exchange of labeled water (20). In cells with highly permeable membranes, higher values for P_d are more often found by the NMR method (5, 6) than by other techniques. The only reliable estimate of P_d, using non-NMR techniques, was made by Gutknecht (24) for internally perfused cells of Valonia, and after correction for the effect of extracellular unstirred layers, a value of $P_d = 2.36 \times 10^{-4} \, cm \, s^{-1}$ was obtained. Such a correction can be done only for single-celled systems with a low water

permeability and this experiment could certainly not be performed with tissues. Isotope exchange techniques measure the total exchange of water between the root and its surroundings, i.e., the diffusion of the water molecules through the entire extracellular space of the root (Fig. 1) is included in the exchange process. The technique applied in this work eliminates this problem because the paramagnetic ions are inside the extracellular space and the protons of water molecules are relaxed as soon as they reach the outer surface of the membrane. The discrepancy in P_d between NMR and isotope exchange data indicates that the previously reported values of τ_a (20, 25) are influenced by the time required for water to move through the extracellular space of the root (including cell walls). Our value of P_d for maize cortical cells is higher than the values found by the NMR method for Nitella cells ($P_d = 2.5 \times 10^{-3} \, cm \, s^{-1}$ [5]) and Chlorella cells ($P_d = 2.1 \times 10^{-3} \, cm \, s^{-1}$ [6]), but is still lower than for ivy bark cells ($P_d = 3 \times 10^{-2} \, cm \, s^{-1}$ [26]) and for Elodea leaf cells (7), where only a lower limit of $P_d > 3 \times 10^{-2} \, cm \, s^{-1}$ was found.

Although the NMR method eliminates the problem of the extracellular unstirred layer, the question of whether or not water permeation through the plasmalemma membrane is the rate-controlling step of the water exchange process still remains. For P_d to be the limiting factor in intra-extracellular water exchange, $\tau_D < \tau_a$, where τ_D is the time taken by a water molecule to diffuse a distance approximately equal to the cell radius, i.e., from vacuole through tonoplast, cytoplasm, and plasmalemma to reach the cell wall, where the relaxation at paramagnetic centers takes place. Using $\tau_D = r^2/2D_w$ and with a diffusion coefficient of $D_w \sim 1 \times 10^{-5} \, cm^2 \, s^{-1}$, we obtained $\tau_D = 200$ ms, which is comparable with τ_a calculated from Eq. 1. An analysis of the intracellular diffusion problem for model cells of different shapes was performed by Stout et al. (7) to determine the controlling factor of water exchange. According to this procedure, our water-exchange time for maize cortical cells is controlled by both membrane water permeability and internal unstirred layers, and a slightly higher value for $P_d = 8 \times 10^{-3} \, cm \, s^{-1}$ was obtained. The above calculations require the exact value of the self-diffusion coefficient of the intracellular water. The complex anatomy of plant cell (water in cytoplasm and vacuole) makes this impossible, hence it is difficult to make a definite statement about the controlling factor by this approach.

A potential source of error in estimating P_d could be the alteration of the membrane water permeability by paramagnetic ions. A detailed study of water exchange across the red cell membrane (4) showed that high $MnCl_2$ concentrations (25–50 mM) can induce a systematic error of 35–45% in the estimation of the τ_a. It seems that in plant systems high Mn^{2+} concentrations do not alter the permeability of membranes to water for following reasons.

(a) T_1 was independent of external $MnCl_2$ concentrations from 5 to 50 mM (Fig. 10). Stout et al. (6, 7) also

found that τ_a for Chlorella cells and Elodea leaf cells was independent of $MnCl_2$ concentrations in the range 0.025–30 mM and 10–80 mM, respectively. It was found (26), however, that τ_a of ivy bark could be affected by Mn^{2+}, but only for concentrations higher than 50 mM. The same value of T_1 (plateau in Fig. 10) was obtained for roots treated with $MnCl_2$ and Mn-EDTA; Figs. 5 and 6 show that the uptake curves have a similar shape for both. This could be explained only if both agents were toxic (which is very unlikely for Mn-EDTA) or if neither changed the membrane properties within the concentration range studied here.

(b) The water content of the maize root was unaltered during treatment with solutions of $MnCl_2$ and Mn-EDTA in the whole concentration range.

(c) Finally, in the presence of 10 mM^{-3} $MnCl_2$ cell membranes of barley root were not disrupted by Mn^{2+} (13) nor was the respiration of rice seedlings affected (11) even after prolonged treatment (several hours).

Let us now return to the nature of the multiphase absorption curve on Fig. 4. The biphasic time course of Mn^{2+} uptake with the transition point at ~70 min was observed for rice roots (11) and for oat roots (21). It was suggested that such a biphasic pattern is related to the structural diversity of the root (e.g., cortex, stele). We concluded earlier that region A in Fig. 4 corresponds to the saturation of the extracellular space of the root. Having entered the apoplast, ions (Mn^{2+}, Mn-EDTA^{2-}) must traverse some membrane (Fig. 1) since the Casparian strip effectively blocks the cell wall apoplast. Fortunately, it is possible to separate the stele from the cortex. It is evident from Figs. 5 and 6 that ions simultaneously appear in the cortical cells and in the stele. This could be the explanation for the biphasic uptake, but in long-term experiments a third transition was observed (Fig. 4). Therefore, we relate the multiphasic pattern to different cellular compartments. The cortical and stelar symplasm are continuous through the endodermis, and region B (Fig. 5) was hypothesized to be due to the influx of manganese ions into the cytoplasmic continuum of the root and translocation to the shoot. The symplasmic transport essentially bypasses vacuoles (22). Fig. 7 shows that manganese appears in the leaves at the beginning of the region B (Fig. 5) and its concentration continuously increases, which indicates that the manganese is rapidly carried through the plant vascular system. In studies of uptake of K^+ and Na^+ ions by barley roots, Pitman (27) showed that transport through the cells was more rapid than was possible by diffusion through the apoplast. An initial accumulation of Mn^{2+} up to saturation was also observed in rice roots, after which the ions were directly transported to the shoot (11).

The third phase of absorption (region C) represents the large influx of manganese ions into the vacuoles of the root. If we compare the absolute amounts of manganese (Fig. 4 a) and $1/T'_{1b}$ (Fig. 4 b) in roots at all three plateaus, their ratio corresponds to the relative ratio of the vacuole to the

other parts of a cell. It was recently reported (28), from an effect of Mn^{2+} ions on the broadening of lines in the ^{32}P NMR spectrum of maize root tips that Mn^{2+} is preferentially transported to vacuoles after a 1.75 h loading period. The tip differs significantly in its structural characteristics from the main part of a primary root (29) and this will certainly produce different dynamics of the ion transport.

The above explanation of multiphase absorption is further confirmed by analysis of half-times for saturation of particular cellular compartments. Our measurements revealed that $t_{1/2}$ for saturation of the surface film, extracellular space, cytoplasm, and vacuole with Mn^{2+} are 0.2, 6.2, 78, and 1,000 min, respectively, while 0.3, 14, 74, and 2,919 min was found for radioactive $^{28}Mg^{2+}$ in onion roots (23).

If our explanation of the multiphase absorption of manganese by the root is correct, the fast and slow relaxing components of the root water (region B in Figs. 5 and 6) could be attributed to cytoplasmic (T'_{1a}) and vacuolar (T'_{1b}) water. Fig. 11 shows that $1/T'_{1a}$ is a linear function of internal concentration of paramagnetic ions, and T'_{1a} is more sensitive to the concentrational changes than T'_{1b}. Therefore, we conclude that paramagnetic ions inside the cytoplasm induce fast relaxation of cytoplasmic water protons and that vacuolar relaxation is due to the water exchange through the tonoplast membrane to the fast relaxing cytoplasmic region. The two components are observed due to the effect of Mn^{2+} or Mn-EDTA^{2-} ions inside the cytoplasm, which reduce the relaxation time of cytoplasmic water so much that T_{1a} becomes shorter than the water exchange time between the two compartments. A linear change of $1/T'_{1b}$ with manganese concentration would be due to the backflux term being decreased by increased concentrations of Mn-EDTA^{2-} inside the cytoplasm. The splitting of the root T_1 into two components was not observed for external concentrations of Mn-EDTA lower than 25 mM (Fig. 11), which means that cytoplasmic concentrations of Mn-EDTA are insufficient to gener-
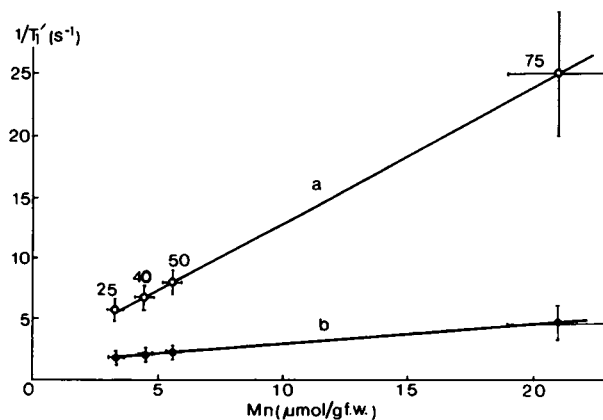

FIGURE 11   The relaxation rates $1/T'_1$ for fast (a) and slow (b) relaxing component vs. manganese content of the root (Tabe II). Numbers on the lines are concentrations of external Mn-EDTA solutions in mM.

ate two T_1 components, i.e., water exchange through the tonoplast is fast enough to average the vacuolar and cytoplasmic water into a single T_1.

It was shown (4, 30) that measured amplitudes of fast and slow component (P'_a and P'_b) need not equal the actual population size (P_a and P_b), but $P'_a = 32–35\%$ and $P'_b = 65–68\%$ for maize root are close to the real anatomical compartmentalization of cellular water in the typical root cell (29). Two proton relaxation times with $P'_a \sim 30\%$ and $P'_b \sim 70\%$ were found in maize leaves treated with $MnSO_4$ solutions (31) and in ivy bark cells (26), but P'_a and P'_b were attributed to hydration water and the intracellular bulk water, respectively, ignoring compartmentalization of plant cells. This is contradictory to our assignment of water compartments only at first sight, since it must be remembered that the cytoplasmic water strongly interacts with macromolecules and subcellular organeles present in this compartment. On the other hand, the vacuolar sap is a relatively diluted solution of ions and vacuolar water and, therefore, could be safely considered bulk water.

The effect of dissolved paramagnetic ions on the proton relaxation rate, R_1, of solvent water is expressed by a classical relation (32)

$$R_1 = 1/T_1 = \frac{12\pi^2\gamma^2\mu_{ion}^2}{5kT}\eta N_{ion} = C\frac{\eta}{T}N_{ion}, \qquad (3)$$

where η is the solution viscosity, T is the absolute temperature, and N_{ion} is the ion concentration per cm^3. It seems that metal-EDTA complexes are transported in plant as a single entity (22). If we compare $1/T_{1e}$ vs. manganese concentration for aqueous solutions of $Mn-EDTA^{2-}$ with the same dependence shown in Fig. 11 for maize roots ($T = $ constant), the apparent viscosity of root cells cytoplasms was about 2 times larger than in the aqueous solutions. The same value was recently obtained for the frog muscle cytoplasm using pulsed-gradient ^{31}P NMR technique (33). Eq. 3 could not be applied to Mn^{2+} inside the cytoplasm since Mn^{2+} ions are partially bound (34).

As can be seen from Figs. 4–6 the relaxation rate of root water protons could be taken as an indicator of the manganese content of the root. Therefore, the absorption of manganese by plants could be studied by proton NMR and we believe that this method has some advantages over the classical methods. (a) The measuring procedure is completely non-destructive, i.e., it allows one to follow the whole time course of uptake on a single sample, (b) it is rapid, and (c) the analysis of the relaxation decay could give additional information about the actual distribution of ions within the tissue. Manganese is a micronutrient, and the relatively high concentrations used to study the water exchange are certainly not relevant for normal plant behavior. Preliminary experiments at lower concentrations, e.g., 7×10^{-5} mM and data in the literature (31) show that the method is sensitive enough at concentrations far below 1 mM. The restriction of the method, however, is that it covers paramagnetic ions only.

REFERENCES

1. House, C. R. 1974. Water Transport in Cells and Tissues. Arnold Publishers Ltd., London. 152–192.
2. Conlon, T., and R. Outhred. 1972. Water diffusion permeability of erythrocytes using a nuclear magnetic resonance technique. *Biochim. Biophys. Acta.* 288:354–361.
3. Ratković, S. 1981. NMR studies of water in biological systems at different levels of their organization. *Sci. Yugosl.* 7:19–54.
4. Pirkle, J. L., D. L. Ashley, and J. H. Goldstein. 1979. Pulse nuclear magnetic resonance measurements of water exchange across the erythrocyte membrane employing a low Mn concentration. *Biophys. J.* 25:389–406.
5. Ratković, S., and G. Bačić. 1980. Water exchange in Nitella cells: A PMR study in the presence of paramagnetic Mn^{2+} ions. *Bioelectrochem. Bioenerg.* 7:405–412.
6. Stout, D. G., P. L. Steponkus, L. D. Bustard, and R. M. Cotts. 1978. Water permeability of Chlorella cell membranes by nuclear magnetic resonance. Measured diffusion coefficients and relaxation times. *Plant Physiol. (Bethesda).* 62:146–151.
7. Stout, D. G., R. M. Cotts, and P. L. Steponkus. 1977. The diffusional water permeability of Elodea leaf cells as measured by nuclear magnetic resonance. *Can. J. Bot.* 55:1623–1631.
8. Ohgushi, M., K. Nagayama, and A. Wada. 1978. Dextrane-magnetite: A new relaxation reagent and its application to T_2 measurements in gel systems. *J. Magn. Reson.* 29:599–601.
9. Tanton, T. W., and S. H. Crowdy. 1972. Water pathways in higher plants. II. Water pathways in roots. *J. Exp. Bot.* 23:600–613.
10. Brading, A. F., and A. W. Jones. 1969. Distribution and kinetics of CoEDTA in smooth muscle, and its use as an extracellular marker. *J. Physiol. (Lond.).* 200:387–401.
11. Ramani, S., and S. Kannan. 1975. Manganese absorption and transport in rice. *Physiol. Plant.* 33:133–137.
12. Tiffin, L. O. 1976. Translocation of manganese, iron, cobalt, and zinc in tomato. *Plant Physiol. (Bethesda).* 42:1427–1432.
13. Maas, E. V., D. P. Moore, and B. J. Mason. 1968. Manganese absorption by excised barley roots. *Plant Physiol. (Bethesda).* 43:527–530.
14. Bowen, J. E. 1981. Kinetics of active uptake of boron, zinc, copper, and manganese in barley and sugarcane. *J. Plant Nutr.* 3:215–223.
15. Bačić, G., B. Božović, and S. Ratković. 1978. Proton magnetic relaxation in plant cells and tissues. Effects of external ion concentration on spin-lattice relaxation time (T_1) and water content in primary roots of Zea mays. *Stud. Biophys.* 70:31–43.
16. Ratković, S., G. Bačić, Č. Radenović, and Ž. Vučinić. 1982. Water in plants: a review of some recent NMR studies concerning the state and transport of water in leaf, root and seed. *Stud. Biophys.* 91:9–18.
17. Sillen, L. G., and A. E. Martell. 1964. Stability Constants of Metal-ion Complexes. The Royal Society of Chemistry, London. 638.
18. Läuchli, A. 1976. Apoplasmic transport in tissues. *In* Transport in Plants II, Part B, Tissues and Organs. U. Lüttge, and M. G. Pitman, editors. Springer-Verlag, Berlin. 3–29.
19. Crank, J. 1956. The Mathematics of Diffusion. Oxford University Press, London.
20. Jarvis, P., and C. R. House. 1967. The radial exchange of labeled water in maize roots. *J. Exp. Bot.* 18:695–706.
21. Page, E. R. 1961. Location of manganese taken up in short-term absorption by oat roots. *Nature (Lond.).* 189·597.
22. Anderson, W. P. 1976. Transport through roots. *In* Transport in Plants II, Part B, Tissues and Organs, U. Lüttge and M. G. Pitman, editors. Springer-Verlag, Berlin. 129–151.

23. Maclon, E. A. S., and A. Sim. 1976. Cortical cell fluxes and transport to the stele in excised root segments of Allium cepa L. III. Magnesium. *Planta.* 128:5–9.

24. Gutknecht, J. 1967. Membranes of *Valonia ventricosa:* apparent absence of water-filled pores. *Science (Wash, DC).* 158:787–788.

25. Bačić, G., and S. Ratković. 1982. A near-infrared study of H_2O-D_2O exchange in maize root. *Period. Biol.* 84:111–114.

26. Stout, D. G., P. L. Steponkus, and R. M. Cotts. 1978. Nuclear magnetic relaxation times and plasmalemma water exchange in ivy bark. *Plant Physiol. (Bethesda).* 62:636–641.

27. Pitman, M. G. 1965. Sodium and potassium uptake by seedlings of *Hordeum vulgare. Aust. J. Biol. Sci.* 18:10–24.

28. Kime, M. J., R. G. Ratcliffe, and B. C. Loughman. 1982. The application of ^{31}P nuclear magnetic resonance to higher plant tissue. II. Detection of intracellular changes. *J. Exp. Bot.* 33:670–681.

29. Nobel, P. S. 1974. Biophysical Plant Physiology. W. H. Freeman and Co., San Francisco. Chapter 1.

30. Hazlewood, C. F., D. C. Chang, B. L. Nichols, and D. E. Woessner. 1974. Nuclear magnetic resonance transverse relaxation times of water protons in skeletal muscle. *Biophys. J.* 14:583–606.

31. Samuilov, F. D., V. I. Nikiforova, and E. A. Nikiforov. 1979. Study of the effect of paramagnetic admixtures on spin-lattice relaxation of intracellular water protons. *Biofizika.* 24:270–273.

32. Andrew, E. R. 1958. Nuclear Magnetic Resonance. Cambridge University Press, London. 127.

33. Yoshizaki, K., Y. Seo, H. Nishikawa, and T. Morimoto. 1982. Application of pulsed-gradient ^{31}P NMR on frog muscle to measure the diffusion rate of phosphorus compounds in cells. *Biophys. J.* 38:209–211.

34. White, M. C., F. D. Baker, R. L. Chaney, and A. M. Decker. 1981. Metal complexation in xylem fluid. II. Theoretical equilibrium model and computational computer program. *Plant Physiol. (Bethesda).* 67:301–310.